

# Large-Scale, Low-Energy Excitations in the Two-Dimensional Ising Spin Glass

A. K. Hartmann<sup>1,2,\*</sup> and A. P. Young<sup>2,†</sup>

<sup>1</sup>*Institute for Theoretical Physics, University of Göttingen, 37073 Göttingen, Germany*

<sup>2</sup>*Department of Physics, University of California, Santa Cruz, California 95064*

(Dated: November 5, 2018)

We study large-scale, low-energy excitations in the Ising spin glass with Gaussian interactions in two-dimensions at zero temperature, using an optimization algorithm to determine exact ground states. Periodic boundary conditions are applied. Our results for the fractal dimension of the surface,  $d_s$ , and stiffness exponent,  $\theta'$ , for “droplet” excitations, are in reasonable agreement with estimates from “domain wall” calculations, and so support the predictions of the “droplet theory”. Restricting our analysis to small lattices, we do not find an effective value of  $\theta'$  close to  $-0.47$  as has been recently proposed. The effects of averaging over droplets of different sizes are studied and are also found to be too small to give  $\theta' \approx -0.47$  for smaller sizes. Larger corrections to finite-size scaling would be needed in three and four dimensions in order for the numerical data used to support the “TNT” scenario to be compatible with the droplet theory prediction that the stiffness exponent is the same for droplets and domain walls.

PACS numbers: 75.50.Lk, 75.40.Mg, 05.50.+q

## I. INTRODUCTION

Despite extensive studies over many years, there is still no consensus on the nature of the spin glass state. According to the “droplet picture”<sup>1,2,3,4</sup> the lowest energy excitation, or droplet, of linear size  $l$  containing a given site has a characteristic energy of order  $l^\theta$  where  $\theta$  is a “stiffness” exponent. Droplets are expected to be compact but with a surface which has a non-trivial fractal dimension  $d_s$ , less than the space dimension  $d$ . For Ising spins, the only case considered here, the spin glass state persists to finite temperature for  $d \geq 3$ , and in this situation one has  $\theta > 0$ . On the other hand if the transition is at  $T = 0$ , as happens in  $d = 2$ , then  $\theta < 0$ . A common way to determine  $\theta$  is to compute the characteristic change in the ground state energy when the boundary conditions in one direction are changed from periodic to anti-periodic, which induces a domain wall across the system. Although the domain wall, which stretches across the system from one side to the other, is different geometrically from a droplet, which closes on itself, the droplet picture makes the plausible assumption that the energy varies with length scale in the same way for the two types of excitation. “Domain-wall” calculations give  $\theta$  about 0.20 in three-dimensions<sup>5,6,7,8</sup>, and about 0.70 in four dimensions<sup>9,10</sup>. In  $d = 2$ , a range of domain wall calculations<sup>5,11,12,13,14,15</sup> give  $\theta$  about  $-0.28$ , see Table I, which also shows that the best estimates for  $d_s$  are around 1.27.

In the alternative scenario, known as “replica symmetry breaking” (RSB), it is assumed that the Parisi theory<sup>18,19,20,21</sup> of the infinite range Sherrington-Kirkpatrick model, applies, at least in part, to short range systems. In this picture, the energy of droplets containing a finite fraction of the system does not increase with increasing system size. Although, to our knowledge, there are no calculations of the domain wall energy within the RSB picture, there seems to be no reason why

Reference	$\theta$	$d_s$
Bray and Moore <sup>5</sup>	$-0.294 \pm 0.009$	—
McMillan <sup>11</sup>	$-0.281 \pm 0.005$	—
Rieger et al. <sup>12</sup>	$-0.281 \pm 0.002$	$1.34 \pm 0.10$
Palassini and Young <sup>13</sup>	$-0.285 \pm 0.020$	$1.30 \pm 0.08$
Hartmann and Young <sup>14</sup>	$-0.282 \pm 0.002$	—
Carter et al. <sup>15</sup>	$-0.282 \pm 0.003$	—
Bray and Moore <sup>16</sup>	—	$1.26 \pm 0.03$
Middleton <sup>17</sup>	—	$1.27 \pm 0.01$

TABLE I: Values of the stiffness exponent  $\theta$  and surface fractal dimension  $d_s$  for “domain-wall” calculations in two dimensions. The estimates for  $\theta$  are consistently close to  $-0.28$ , which we shall take to be the correct value (to two decimal places) for the purposes of this article. The most accurate estimates of  $d_s$  are those of Bray and Moore<sup>16</sup>,  $1.26 \pm 0.03$ , and Middleton<sup>17</sup>,  $1.27 \pm 0.01$ .

it should vanish. Hence, it appears that different “ $\theta$ -like” exponents are needed for domain walls and droplets within the RSB picture. To allow for this possibility we will denote by  $\theta$  the exponent for the energy of domain walls and by  $\theta'$  the exponent for droplets. Thus, in this notation, RSB gives  $\theta' = 0$ . Furthermore, in RSB, the surface of the large-scale, low-energy excitations are expected to fill space and so have the fractal dimension  $d_s = d$ . This means that the distributions of both the “spin overlap” and “link overlap”, defined in Sec. II below, are “non-trivial”, in the sense that they have a finite width in the thermodynamic limit, as opposed to the droplet picture in which they both become “trivial”, i.e. are just delta functions, in this limit.

Recently, an intermediate scenario, known as TNT (for “Trivial, Non-Trivial”), has been proposed<sup>22,23</sup>, based on numerical work in  $d = 3$  and 4 at zero temperature. In this picture one has  $\theta' \simeq 0$  ( $< \theta$ ), as in RSB, but

$d_s < d$ , as in the droplet picture. Subsequently, support for the TNT picture was found from finite- $T$  Monte Carlo simulations<sup>24</sup>. However, it has also been criticized by Marinari and Parisi<sup>25</sup> who argued that  $d_s = d$  (in which case one obtains RSB). In addition, Middleton<sup>17</sup> has criticized TNT in the opposite sense by arguing that averaging over droplets of different sizes, which was carried out in Refs. 22 and 23, leads to an incorrect value of  $\theta$  for the small sizes studied, and that asymptotically  $\theta' = \theta$ , so the droplet theory is correct.

Moore<sup>26</sup> has also argued that Refs. 22 and 23 obtained the result  $\theta' \simeq 0 (< \theta)$ , rather than  $\theta' = \theta$ , because corrections to scaling were neglected. However, the corrections that Moore considers are different. He argues that there is a sub-leading (repulsive) contribution to the energy of a droplet, varying as  $l^{-\omega}$ , which arises because the wall cannot intersect itself. The amplitude of this contribution is argued to be larger for a droplet, since this has to return to its original location, than for a domain wall which does not have to do this and so would have less tendency to intersect itself. Moore argues that evidence for this contribution to the droplet energy is found in the work of Lamarcq et al.<sup>27</sup>, who compute the energy of droplets in three dimensions by determining the minimum energy excitation above the ground state which contains a given number of spins including one fixed central spin. Moore further argues that a combination of this repulsive piece of the droplet energy which decreases with increasing size  $l$ , and the leading  $l^\theta$  term which increases with increasing  $l$ , can give a droplet energy which is roughly constant for the small range of droplet sizes studied numerically. By contrast, for domain walls, the amplitude of the repulsive correction is argued to be small, and so the correct asymptotic value of  $\theta'$  (i.e.  $\theta$ ) would be observed even for small sizes.

Further motivation for Moore's ideas comes from results in  $d = 2$ , where a much larger range of system sizes  $L$  can be studied than in higher dimensions. While  $T = 0$  domain-wall calculations give  $\theta$  about  $-0.28$  as noted above, both finite- $T$  simulations<sup>28,29</sup> and  $T = 0$  studies in a magnetic field<sup>30</sup>, both of which excite droplets rather than domain walls, find  $\theta$  about  $-0.47$ . A good review of this situation is given in Ref. 31. Since  $\theta < 0$  in  $d = 2$ , both the  $l^\theta$  and  $l^{-\omega}$  contributions to the droplet energy decrease with increasing  $L$  but, Moore argues, could combine to give an effective exponent of about  $-0.47$  for small  $l$  crossing over to the asymptotic value of about  $-0.28$  for larger sizes. A different perspective on these results has in two dimensions been given by Kawashima<sup>32</sup>, who argues that  $\theta' \simeq -0.47$  is the *asymptotic* value for droplets and different from  $\theta$  obtained from domain wall calculations. Recently, Picco et al.<sup>33</sup> have studied the first excited state, as well as the ground state, in a  $2-d$  spin glass, and from their results they infer that  $\theta' \simeq -0.46$ .

With current algorithms<sup>34</sup>, it does not seem possible to push numerical studies in  $d = 3$  to significantly larger sizes than has already been done. However, in  $d = 2$ , there are more efficient algorithms as we shall see, which

allow larger sizes to be considered, and the goal of the present paper is to investigate large-scale, low-energy excitations in two-dimensions at  $T = 0$  by the approach of Ref. 23, described below. While Middleton<sup>17</sup> has also applied the method of Ref. 23 to  $d = 2$ , our work differs from his because we use periodic boundary conditions, as opposed to the ‘‘open, with boundary spins fixed under perturbation’’ or ‘‘link periodic’’ boundary conditions used by Middleton. Since they have no surface, samples with periodic boundary conditions are expected to have relatively small finite-size corrections. Our choice of boundary conditions is discussed more fully in Sec. III. In addition, we also perform an analysis in which we just look at the large droplets generated, for each lattice size, rather than averaging over droplet sizes.

Our motivation is to understand in detail finite-size scaling for spin glasses in two dimensions. This should give better insights into finite-size scaling in higher dimensions, and may help us understand whether the result that  $\theta' < \theta$  found in three and four dimensions is real or simply caused by corrections to scaling. More precisely, by studying Ising spin glass ground states in  $d = 2$  we aim to:

- (i) separate out the effects of averaging over different droplet sizes, to see how this influences the values of  $\theta$  and  $d_s$  for a system in two-dimensions with periodic boundary conditions, and
- (ii) look for the crossover, expected by Moore<sup>26</sup>, from  $\theta$  about  $-0.47$  to about  $-0.28$ .

We consider a continuous (Gaussian) distribution of interactions to avoid the additional complications coming from the degenerate ground state in the  $\pm J$  model<sup>14,35</sup>.

The model and the technique to generate excitations used in Ref. 23 is described in Sec. II. Our choice of boundary conditions is discussed in Sec. III. The results are presented in Sec. IV and the conclusions summarized in Sec. V.

## II. THE MODEL AND TECHNIQUE

The Hamiltonian is

$$\mathcal{H} = - \sum_{\langle i,j \rangle} J_{ij} S_i S_j, \quad (1)$$

where the sum is over nearest neighbor pairs of sites on a square lattice, the  $S_i$  are Ising spins taking values  $\pm 1$ , and the  $J_{ij}$  are Gaussian variables with zero mean and standard deviation unity. The lattice contains  $N = L \times L$  sites. The techniques presented below work for several kinds of boundary conditions, but our results will be mainly for periodic boundary conditions.

We find the large-scale, low energy excitations out of the ground state by following the procedure of Ref. 23. First of all we compute the ground state and denote the spin configuration by  $S_i^{(0)}$ . We then add a perturbation

to the Hamiltonian designed to increase the energy of the ground state relative to the other states, and so possibly induce a change in the ground state. This perturbation, which depends upon a positive parameter  $\epsilon$ , changes the interactions  $J_{ij}$  by an amount proportional to  $S_i^{(0)}S_j^{(0)}$ , i.e.

$$\Delta\mathcal{H}(\epsilon) = \epsilon \frac{1}{N_b} \sum_{\langle i,j \rangle} S_i^{(0)} S_j^{(0)} S_i S_j, \quad (2)$$

where  $N_b = dN$  is the number of bonds in the Hamiltonian. In the numerical work we took  $\epsilon = 2$ .

The energy of the ground state will thus increase exactly by an amount  $\Delta E^{(0)} = \epsilon$ . The energy of any other state,  $\alpha$  say, will increase by the lesser amount  $\Delta E^{(\alpha)} = \epsilon q_l^{(0,\alpha)}$ , where  $q_l^{(0,\alpha)}$  is the ‘‘link overlap’’ between the states ‘‘0’’ and  $\alpha$ , defined by

$$q_l^{(0,\alpha)} = \frac{1}{N_b} \sum_{\langle i,j \rangle} S_i^{(0)} S_j^{(0)} S_i^{(\alpha)} S_j^{(\alpha)}, \quad (3)$$

in which the sum is over all the  $N_b$  pairs where there are interactions. Note that the *total* energy of the states is changed by an amount of order unity. Fig. 1 shows the variation of the energy of the ground state and that of an excited state which has an energy  $\delta E$  above it in the absence of the perturbation, as a function of the strength of the perturbation. For the value of  $\epsilon$  shown the excited state has become the new ground state.

We denote the new ground state spin configuration by  $\tilde{S}_i^{(0)}$ , and indicate by  $q_l$ , with no indices, the link-overlap between the new and old ground states, i.e.

$$q_l = \frac{1}{N_b} \sum_{\langle i,j \rangle} S_i^{(0)} S_j^{(0)} \tilde{S}_i^{(0)} \tilde{S}_j^{(0)}. \quad (4)$$

Similarly we denote the spin overlap by  $q$ , where

$$q = \frac{1}{N} \sum_i S_i^{(0)} \tilde{S}_i^{(0)}, \quad (5)$$

and the change in ground state energy by  $\Delta E$ , see Fig. 1.

From Fig. (1), we see that the change in ground state energy satisfies the inequalities

$$\epsilon q_l \leq \Delta E \leq \epsilon. \quad (6)$$

Furthermore, the unperturbed excitation energy  $\delta E$  of the state which has become the perturbed ground state (since  $\delta E + \epsilon q_l < \epsilon$ , see Fig. 1) satisfies the conditions

$$0 < \delta E < \epsilon(1 - q_l). \quad (7)$$

Note that

$$1 - q = \frac{2N_{\text{vol}}}{N}, \quad (8)$$

where  $N_{\text{vol}}$  is the number of flipped spins, and

$$1 - q_l = \frac{2N_{\text{surf}}}{N_b}, \quad (9)$$

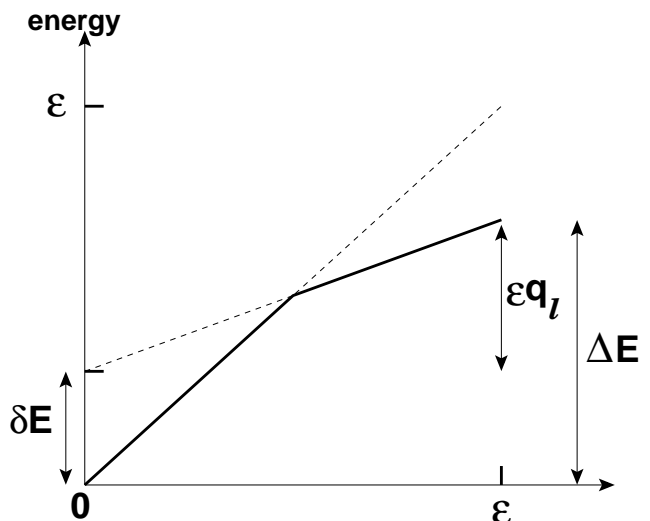


FIG. 1: A sketch of the variation of the ground state and an excited state an energy  $\delta E$  above it, as a function of the strength of the perturbation,  $\epsilon$ . The variation of the ground state energy as a function of  $\epsilon$  is shown by the solid line. For the value of the perturbation indicated, the unperturbed excited state has become the perturbed ground state. We denote by  $\Delta E$  the change in ground state energy due to the perturbation.

where  $N_{\text{surf}}$  is the number of bonds crossed by the domain wall bounding the flipped spins, i.e. the surface of the domain wall.

Next, following Ref. 23, we discuss how quantities like  $q_l$  and  $q$  are expected to vary with system size. Consider first those samples where a large excitation comprising a finite fraction of the sites is generated, e.g. those where  $|q| \leq 0.5$ . The average of  $1 - q$  over these samples given by

$$[1 - q]_{\text{av}}' \sim 1, \quad (10)$$

where  $[\dots]_{\text{av}}$  denotes an average over samples and the prime denotes a restricted average over those samples with  $|q| \leq 0.5$ . From Eq. (9) we see that the average of  $1 - q_l$  over these samples given by

$$[1 - q_l]_{\text{av}}' \sim L^{-\{d-d_s\}}. \quad (11)$$

Such a large excitation costs an energy of order  $L^{\theta'}$ . This must be more than compensated for by the energy gained from the perturbation (relative to the ground state),  $\epsilon(1 - q_l)$ , which, from Eq. (9), is proportional to  $\epsilon L^{-(d-d_s)}$ . Hence, assuming a distribution of droplet energies with a finite weight at the origin, the probability that such a large excitation can be created is given by

$$P(|q| \leq 0.5) \sim L^{-\{\theta'+(d-d_s)\}}. \quad (12)$$

We now consider results of averaging over *all* samples rather than just those with large droplets. Eq. (12) shows that there is probability  $\sim L^{-\{\theta'+(d-d_s)\}}$  to have  $1 - q$

of order unity, and so, assuming that samples with large droplets dominate the average, we have

$$[1 - q]_{\text{av}} \sim L^{-\{\theta' + (d - d_s)\}}. \quad (13)$$

Similarly, we find

$$[1 - q_l]_{\text{av}} \sim L^{-\mu_l}, \quad (14)$$

where

$$\mu_l = \theta' + 2(d - d_s). \quad (15)$$

Note that that the ratio of the quantities in Eqs. (13) and (14) is independent of  $\theta'$ , i.e.

$$R \equiv \frac{[1 - q_l]_{\text{av}}}{[1 - q]_{\text{av}}} \sim L^{-\{d - d_s\}}. \quad (16)$$

Eq. (7) shows that the droplet excitation energy  $\delta E$ , see Fig. 1, scales in the same way as  $1 - q_l$ , i.e. like Eq. (11) if only samples with  $|q| \leq 0.5$  are studied, and like Eq. (14) if all samples are averaged over.

In general we can extract  $d - d_s$  from the surface to volume ratio of the excited droplets of spins, but to get  $\theta'$  we also need information about the *probability* that a large droplet is excited.

### III. CHOICE OF BOUNDARY CONDITIONS

In those two-dimensional models where the bonds form a “planar graph”, which unfortunately excludes periodic boundary conditions in both directions, very efficient polynomial time “matching” algorithms can be used<sup>14,17,34,36,37,38</sup> to determine the ground state. As a result very large sizes can be studied<sup>39</sup>. By contrast, in three or higher dimensions the calculation is known<sup>37</sup> to be NP-hard which means that a polynomial-time algorithm is unlikely to exist.

In Fig. 2 we show the excitation generated, using the matching algorithm, for a  $200 \times 200$  sample with periodic boundary conditions on the vertical edges, and open boundary conditions on the horizontal edges. Unfortunately, the boundary of the resulting excitation is not a droplet but a single domain wall which spans the whole system. This structure would not have been possible if periodic boundary conditions had also been applied along the top and bottom edges. We find that a single domain wall is generated for a significant fraction of the samples with open-periodic boundary conditions, and so these boundary conditions are not appropriate for a study of the *differences* between droplets and domain walls<sup>40</sup>.

One possibility to prevent the occurrence of domain walls is to first generate a ground state with open boundary conditions, and then fix the orientations of the boundary spins<sup>17</sup> relative to each other by introducing very strong bonds in favor of their relative ground-state orientations. This still allows us to use the fast matching

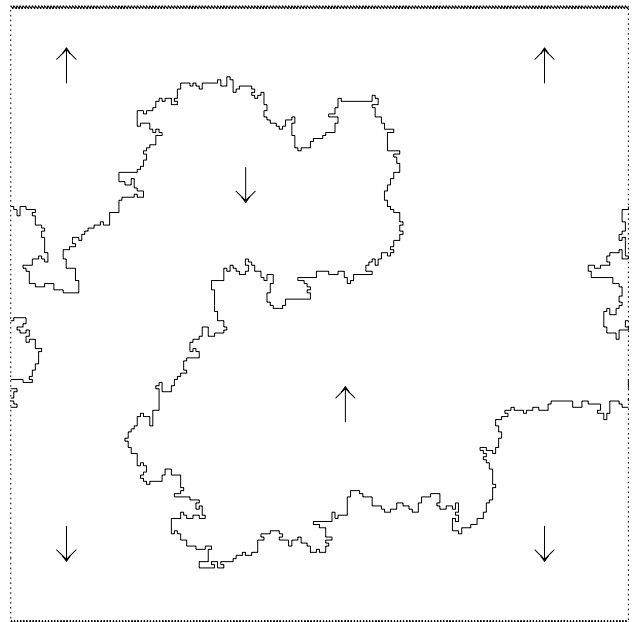


FIG. 2: An excitation generated for an  $L = 200$  system obtained using the matching algorithm. The vertical edges have periodic boundary conditions while the horizontal edges have open boundary conditions. With the matching algorithm it is not possible to have periodic boundary conditions in both directions. The line shows the boundary separating the region where the spins are flipped when the perturbation is applied (denoted by “↓”) from the region where they are not flipped (denoted by “↑”). One sees that, in this case, the excitation is a single domain wall rather than a droplet.

algorithm and hence to treat large system sizes. We have only tested this approach briefly, since we found that usually only very small droplets are generated, with almost none spanning more than one quarter of the system (i.e. with  $|q| \leq 0.5$ ). The reason is that by fixing the boundary spins an effective repulsion of the domain wall from the boundary is introduced. This reduces the sizes of the droplets. Furthermore, it is also likely that this repulsion affects the morphology of the domain walls.

We therefore decided to apply periodic boundary conditions in both directions which, unfortunately, means that the matching algorithm cannot be used<sup>41</sup>. Instead we use the spin glass ground state server at the University of Cologne<sup>42</sup>. This uses a “branch and cut” algorithm for which, as we shall verify, the CPU time increases faster than a power of the system size, so we cannot study such large systems as are possible with the matching algorithm<sup>39</sup>. Nonetheless, the implementation of the branch and cut algorithm on the Cologne server is very efficient, so we can still study quite a large range of sizes, in practice  $L \leq 64$ .

Fig. 3 shows a large droplet excitation created for an  $L = 64$  sample with periodic boundary conditions. In some samples where large-scale excitations are produced, the region of flipped spins wraps round the sample cre-

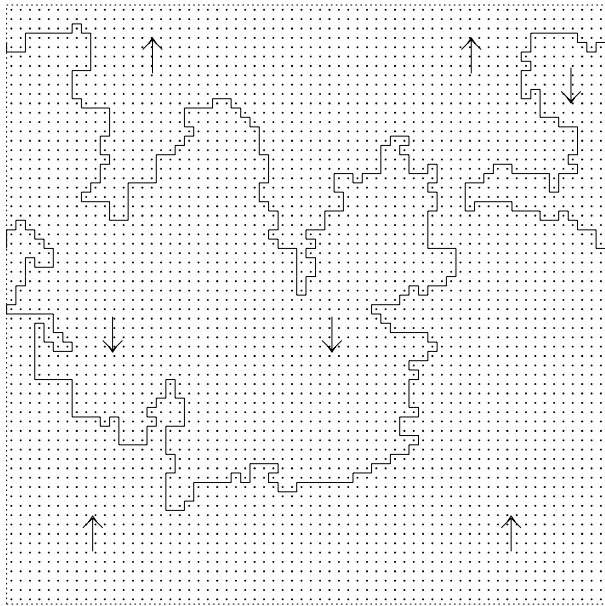


FIG. 3: A droplet excitation generated for an  $L = 64$  system obtained using the branch and cut algorithm of the Cologne spin glass server. Periodic boundary conditions are applied in both directions. The dots indicate the lattice sites. Clearly the region where the spins are flipped forms a droplet.

$L$	4	6	8	12	16	24	32	44	64
$N_{\text{samp}}$	1973	1972	2059	1973	2098	1993	2099	2015	1763

TABLE II: The number of samples  $N_{\text{samp}}$  for each lattice size  $L$ .

ating a “sponge-like” excitation<sup>43,44</sup>, which is, in effect, made up of two domain walls<sup>45</sup>. An example is shown in Fig. 4. Later we will discuss the role played by sponges, finding that their properties are very similar to those of large-scale, non-sponge excitations.

#### IV. RESULTS

All the numerical results are for a strength of the perturbation  $\epsilon = 2$ . Asymptotically, the results should be independent of the value of  $\epsilon$ . However, if we make  $\epsilon$  too large, then the asymptotic behavior will only be seen for large sizes, and if  $\epsilon$  is too small the statistics will be poor. Based on experience with other models<sup>23</sup>, the choice  $\epsilon = 2$  seems to be a reasonable compromise. In Table II we show the number of samples studied for each lattice size.

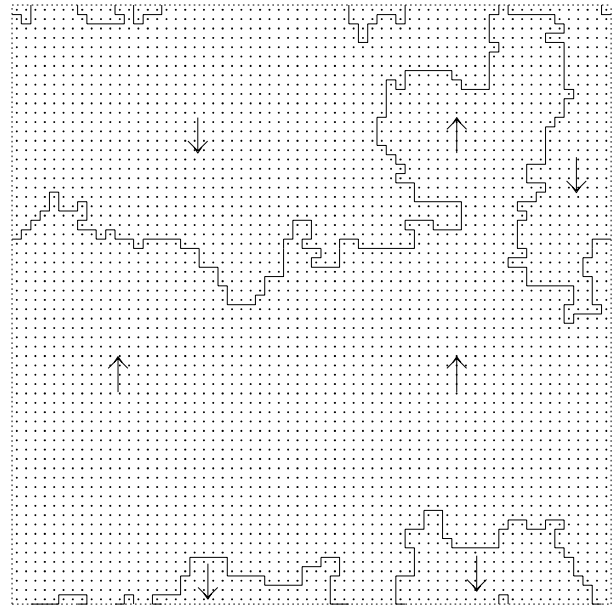


FIG. 4: A “sponge-like” excitation generated for an  $L = 64$  system with periodic boundary conditions in both directions.

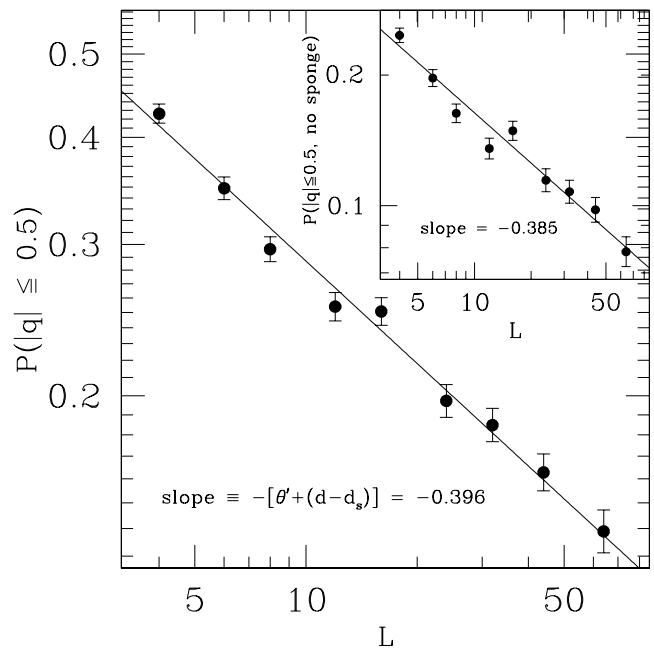


FIG. 5: A log-log plot of the fraction of samples for which the spin overlap between the perturbed and unperturbed ground states satisfies  $|q| \leq 0.5$ . According to Eq. (12) the slope should be  $-\lceil \theta' + (d - d_s) \rceil$ . The inset is a log-log plot of the fraction of samples for which not only is  $|q| \leq 0.5$  but also the excitation is not sponge-like, see Fig. (4). The slope is almost the same as that for in the main part of the figure, indicating that a roughly fixed fraction, about 55%, of excitations with  $|q| \leq 0.5$  are not sponges.

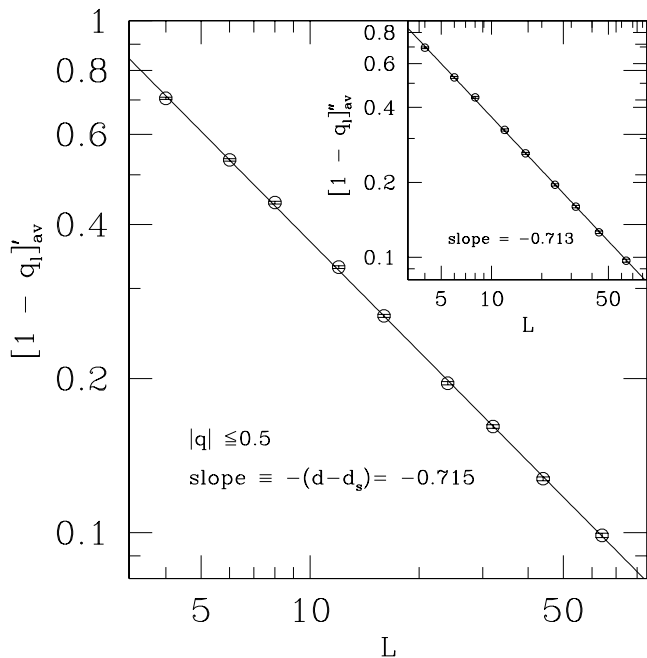


FIG. 6: A log-log plot of the average of  $1 - q_l$  over those samples for which the spin overlap between the perturbed and unperturbed ground states satisfy  $|q| \leq 0.5$ . According to Eq. (11) the slope should be  $-(d - d_s)$ . The inset shows results averaged over samples where not only is  $|q| \leq 0.5$  but also the excitation is not sponge-like, see Fig. 4. The slope is virtually the same as that in the main part of the figure, indicating that sponges have similar properties to large non-sponge, droplet excitations.

### A. Average over samples with large droplets

Firstly, we consider results obtained by averaging only over those samples where large droplets were created, i.e. the spin overlap satisfies  $|q| \leq 0.5$ . Fig. 5 shows results for the probability that this occurs, while Fig. 6 shows the average of  $1 - q_l$  for those samples. Fitting the data according to Eqs. (12) and (11) we find

$$\begin{aligned} d - d_s &= 0.715 \pm 0.003 \\ \theta' + (d - d_s) &= 0.396 \pm 0.015, \end{aligned} \quad (17)$$

which gives

$$\begin{aligned} d_s &= 1.285 \pm 0.003 \\ \theta' &= -0.319 \pm 0.015. \end{aligned} \quad (18)$$

The value of  $d_s$  agrees very well with best estimates of around 1.27, see Table I, while the value of  $\theta'$  is a little more negative than the best estimates for  $\theta$  from domain wall calculations, which is about  $-0.28$ , see Table I. However, the difference is quite small, only about two standard deviations. Hence we see that our results are consistent with the droplet theory being correct in two dimensions.

The insets to Figs. 5 and 6 show data for those samples where the excitation is not only large, i.e.  $|q| \leq 0.5$ , but

	$d_s$	$\theta'$	$Q_1$	$Q_2$
$4 \leq L \leq 64$	$1.285 \pm 0.003$	$-0.319 \pm 0.015$	0.006	0.253
$4 \leq L \leq 16$	$1.299 \pm 0.005$	$-0.288 \pm 0.029$	0.037	0.050
$16 \leq L \leq 64$	$1.285 \pm 0.008$	$-0.298 \pm 0.043$	0.405	0.639

TABLE III: Fits for the data for those samples where  $|q| \leq 0.5$  for different ranges of sizes.  $Q_1$  and  $Q_2$  are the quality factors, as conventionally defined<sup>46</sup>, of the fits for  $[1 - q_l]_{av}$  and  $P(|q| \leq 0.5)$  respectively. Note that  $Q_1$  is quite small for the fit with all sizes. This is because the error bars are small and there are clearly some systematic effects. For example, if we omit the  $L=4$  point then  $Q_1$  becomes 0.129, which is much better. However, this then gives  $\theta = -0.347 \pm 0.019$ , which is further from the accepted value of about  $-0.28$  but agrees within the error bars with the value in the table.

is also not sponge-like, i.e. is *not* of the form shown in Fig. 4. The fraction of samples with  $|q| \leq 0.5$  for which the excitation is not sponge-like is roughly independent of size at about 55%. This is why the slope in the inset to Fig. 5 is very similar to that in the main part of the figure. Furthermore, the slope of the data for the average of  $1 - q_l$  in the inset to Fig. 6 is very similar to the average over all samples with  $|q| \leq 0.5$  (shown in the main part of the figure), indicating that the properties of sponge-like excitation are similar to those of large non-sponge droplets.

We have also analyzed the data including just the smaller sizes,  $4 \leq L \leq 16$ , and just the larger sizes,  $16 \leq L \leq 64$ , and the results are shown in Table III. The values of  $\theta'$  are, given the error bars, scarcely more negative than the best accepted value of  $-0.28$ . One does not see a systematic trend over this range of sizes. In particular we do not see the crossover, expected by Moore<sup>26</sup>, from a value of about  $-0.47$  at smaller sizes to about  $-0.28$  at larger sizes.

From Eq. (7) we expect that the unperturbed excitation energy,  $\delta E$ , of the droplet created by the perturbation, see Fig. 1, should scale in the same way as  $1 - q_l$ , i.e. with an exponent  $d - d_s$  if restrict the average to those samples with  $|q| \leq 0.5$ . The data, plotted in Fig. 7, gives  $d - d_s = 0.683 \pm 0.011$  as compared with  $0.715 \pm 0.003$  obtained from the data for  $1 - q_l$  in Fig. 6. The difference, which is quite small, is presumably due to corrections to scaling.

We should make clear why the average of  $\delta E$  induced by the perturbation varies as  $L^{-(d-d_s)}$  (if we only include samples with  $|q| \leq 0.5$ ), whereas the characteristic droplet energy varies as  $L^{\theta'}$ . The point is that there is a *distribution* of droplet energies which is assumed to have a finite weight at the origin. Thus, some samples will have a large-scale droplet with energy *much less* than  $L^{\theta'}$ . In fact, the perturbed ground state will only have a system-size droplet for those samples where the droplet energy is comparable to the energy which can be gained from the perturbation, i.e.  $L^{-(d-d_s)}$ . The probability of this occurring is therefore  $L^{-\{\theta'+(d-d_s)\}}$ , as shown in

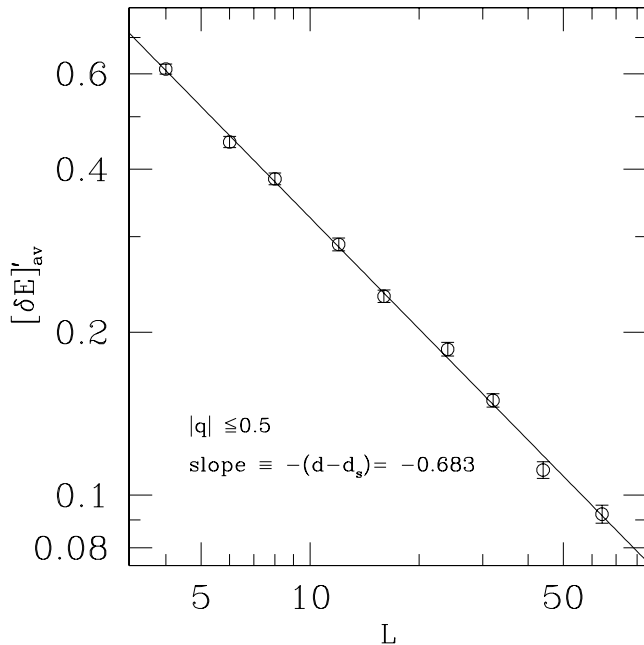


FIG. 7: A log-log plot of the average of the unperturbed excitation energy,  $\delta E$ , see Fig. 1, over those samples for which the overlap between the perturbed and unperturbed ground states satisfies  $|q| \leq 0.5$ . According to Eqs. (7) and (11) the slope should be  $-(d - d_s)$ .

Fig. 5.

Our expectation in looking at samples with  $|q| \leq 0.5$  is that there is a single large droplet which dominates, rather than having several smaller droplets of comparable size, and we have verified that this indeed the case. We have separated out the different droplets for each sample and looked at averages over those *droplets* containing  $N/4$  spins or greater (from Eq. (8) this corresponds to  $|q| \leq 0.5$ ). As an example, for  $L = 64$ , out of 1763 samples, 245 of them had  $|q| \leq 0.5$  and 241 had a single droplet which would give  $|q| \leq 0.5$  by itself. If we repeat the finite-size scaling analysis for these large droplets we find  $d - d_s = -0.715 \pm 0.003$  and  $\theta' + (d - d_s) = -0.392 \pm 0.015$ , in very close agreement with the results in Eq. (17).

### B. Average over all samples

Next we discuss the results obtained by averaging over *all* samples, rather than just those with  $|q| \leq 0.5$ . Fig. 8 shows results for the ratio of the average of  $1 - q_l$  to the average of  $1 - q$ , and Fig. 9 shows results for the average of  $1 - q$ . Fitting the data according to Eqs. (16) and (13) we find

$$\begin{aligned} d - d_s &= 0.674 \pm 0.004 \\ \theta' + (d - d_s) &= 0.320 \pm 0.010, \end{aligned} \quad (19)$$

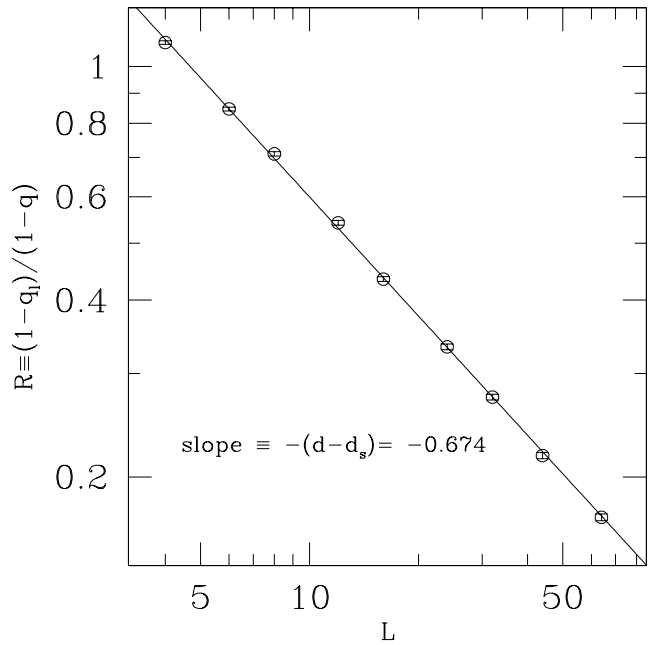


FIG. 8: A log-log plot of the ratio  $[1 - q_l]_{av} / [1 - q]_{av}$  against  $L$  obtained by averaging over *all* samples. From Eq. (16) the slope should be  $-(d - d_s)$ .

which gives

$$\begin{aligned} d_s &= 1.326 \pm 0.004 \\ \theta' &= -0.354 \pm 0.010. \end{aligned} \quad (20)$$

Analyzing the data for different ranges of sizes gives the results shown in Table IV. We note that the values for  $d_s$  are larger than those obtained from analyzing just large droplets, see Table III, and the values for  $\theta'$  somewhat more negative. This is presumably due to the effects of averaging over droplets of different sizes, as discussed by Middleton<sup>17</sup>. Indeed, our results for  $\mu_l \equiv 2(d - d_s) + \theta'$ , see Table IV, agree quite well with those for smaller sizes in Fig. 4 of Ref. 17, even though our boundary conditions are different from his. Nonetheless, the variation of exponents with range of  $L$  is too small to yield  $\theta'$  about  $-0.47$  as suggested by Moore<sup>26</sup>, though the trend ( $\theta'$  more negative for smaller lattice sizes and when we average over different droplet sizes) is in the right direction.

From Table IV, we find  $\theta' = -0.364 \pm 0.021$  when averaging over all samples and just including the smaller sizes. This is about  $-0.08 \pm 0.02$  different from the best value of  $-0.28$ , see Table I. Furthermore, a reanalysis<sup>47</sup> of the data of Ref. 23, just keeping those samples with small  $|q|$ , i.e. similar to our analysis which yielded the fits in Table III, found the same discrepancy in three-dimensions as the original analysis<sup>23</sup> which averaged over droplets of all sizes. We see that the discrepancy in the value for  $\theta'$  in Table III, relative to  $-0.28$ , is much smaller than that in Table IV, even if the fits are restricted to smaller sizes. Hence a much larger effect would be needed in three dimensions to explain why the numerics found

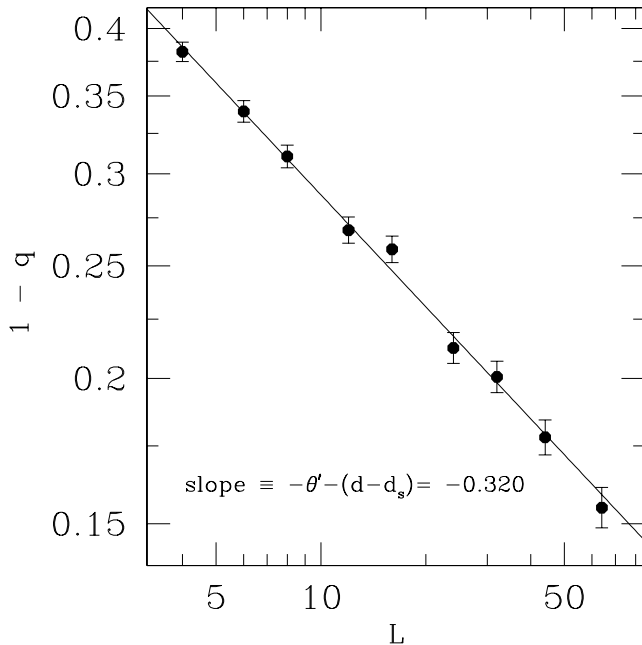


FIG. 9: A log-log plot of  $[1 - q]_{\text{av}}$  against  $L$  obtained by averaging over *all* samples. From Eq. (13) the slope should be  $-\theta' + (d - d_s)$ .

	$d_s$	$\theta'$	$\mu_l$
$4 \leq L \leq 64$	$1.326 \pm 0.004$	$-0.354 \pm 0.010$	$0.995 \pm 0.008$
$4 \leq L \leq 16$	$1.340 \pm 0.007$	$-0.364 \pm 0.021$	$0.956 \pm 0.017$
$16 \leq L \leq 64$	$1.322 \pm 0.011$	$-0.317 \pm 0.030$	$1.039 \pm 0.024$

TABLE IV: Fits for the data obtained by averaging over all samples for different ranges of sizes. Here  $\mu_l \equiv 2(d - d_s) + \theta'$ .

$\theta' \simeq 0$  if the correct result is  $\theta' = \theta \simeq 0.20$ . In four-dimensions there is an even greater discrepancy<sup>23</sup>,  $\theta' \simeq 0, \theta \simeq 0.70$ .

To get an independent estimate of  $d_s$  we have also looked at the size,  $N_{\text{vol}}$ , and surface area,  $N_{\text{surf}}$ , of individual droplets for a given size. Fig. 10 shows data for the largest size  $L = 64$ , and similar results are found for other sizes. Doing a least squares fit gives  $d_s/d = 0.632$ , or  $d_s = 1.264$ , in very good agreement with the best estimates of around 1.27, see Table I.

### C. Computational Complexity

Finally we discuss how the CPU time depends on the system size. Fig. 11 shows a log-log plot of the average CPU-time on the Sun Ultra 10/440 of the Cologne ground state server against  $L$ . The clearly visible upwards curvature indicates that the time increases faster than a power of  $L$ , i.e. the algorithm is non-polynomial, as expected. The inset to the figure shows that, empir-

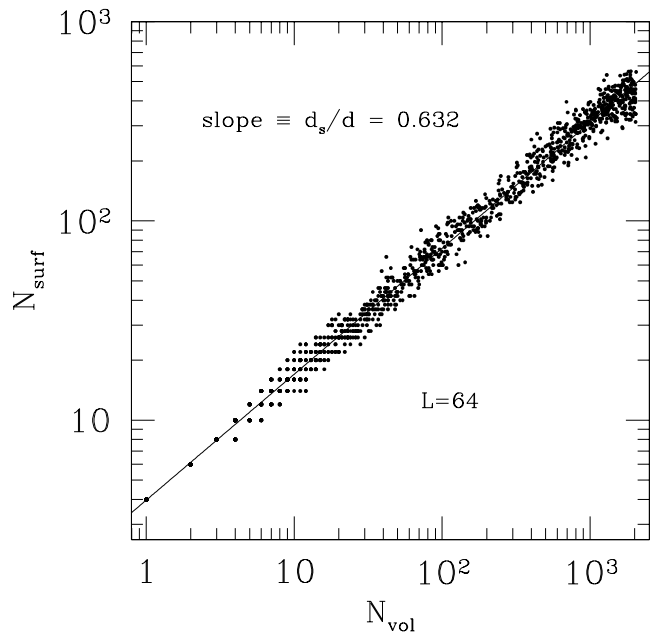


FIG. 10: A plot of the size  $N_{\text{vol}}$  and surface area  $N_{\text{surf}}$  of individual droplets for  $L = 64$ . A fit gives  $d_s/d = 0.632$ .

ically, the CPU time varies like  $\exp(\text{const.} \sqrt{L})$  for the larger sizes studied. However, we do not know the true asymptotic dependence of the CPU time on system size.

## V. CONCLUSIONS

We have studied large-scale, low-energy excitations at  $T = 0$  in the Ising spin glass in two-dimensions with periodic boundary conditions. We have particularly looked at the dependence of  $d_s$  and  $\theta'$  on whether or not we average over droplets of different sizes, and on the range of system sizes that are included in the fits. Averaging just over those samples in which large droplets are generated, see Sec. IV A and Table III, the results do not vary much if we consider different ranges of system sizes, and are consistent with the droplet theory prediction that  $\theta' = \theta$ . If we average over all samples, see Sec. IV B and Table IV, which, for each lattice size, involves averaging over a range of droplet sizes, the results vary more as a function of the range of system size considered. However, the effect is too small to give an effective value of  $\theta'$  close to  $-0.47$  as has been recently proposed<sup>26</sup>, though our result in line 2 of Table IV does lie between  $-0.47$  and the expected value of about  $-0.28$ . It is possible that different ways of generating droplets will yield different effective values of  $\theta'$  for small sizes, and this may be the reason why Refs. 28,29,30 find  $\theta' \simeq -0.47$ .

We have also considered the role of sponge-like excitations, see Fig. 4, finding that their properties are very similar to those of large, non-sponge droplets, see Fig. 3.

Overall, our results support the droplet theory for the



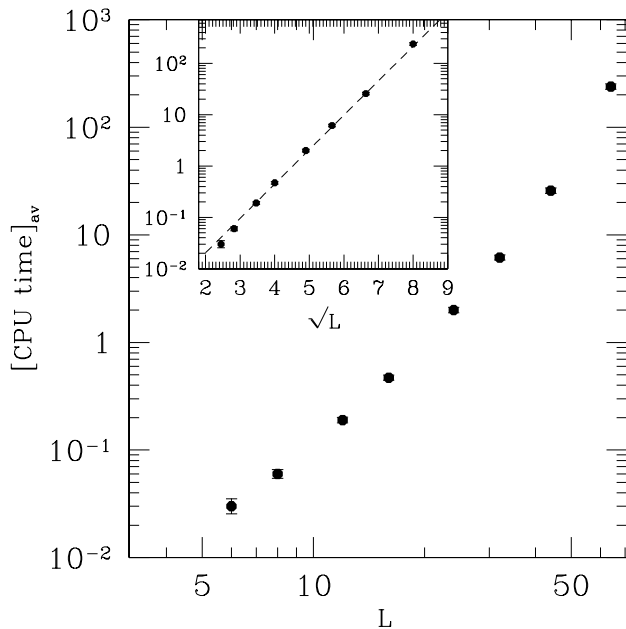


FIG. 11: A log-log plot of the average CPU time per sample as a function of the system size  $L$ . The upwards curvature shows that the CPU time increases faster than a power of  $L$  as expected. The inset shows that the CPU varies roughly as  $\exp(\text{const.} \sqrt{L})$  for the larger sizes. The dashed line is a guide to the eye.

two-dimensional spin glass and do not provide a straightforward way to reconcile the numerical results<sup>22,23</sup> used

to support the TNT scenario with the prediction of the droplet theory that the stiffness exponent is asymptotically the same for droplets and domain walls. For this prediction to be true, larger corrections to finite-size scaling would be needed in three and four dimensions than in two dimensions.

### Acknowledgments

We would like to thank M. A. Moore for a fruitful correspondence and for comments on an earlier version of the manuscript. We would also like to thank A. A. Middleton, M. Palassini, D. A. Huse and F. Ritort for comments on earlier drafts. APY acknowledges support from the National Science Foundation under grant DMR 0086287 and the EPSRC under grant GR/R37869/01. He would also like to thank David Sherrington for hospitality during his stay at Oxford. AKH obtained financial support from the DFG (Deutsche Forschungsgemeinschaft) under grants Ha 3169/1-1 and Zi 209/6-1. We are extremely grateful to the group of Michael Jünger at the University of Cologne for putting their spin glass ground state server in the public domain, and for not complaining even when we used a substantial amount of computer time on it. We would particularly like to thank Thomas Lange and Frauke Liers for helpful correspondence on the use of the server. Also computer resources from the Paderborn Center for Parallel Computing (Germany) and the Institut für Theoretische Physik of the Universität Magdeburg (Germany) were used.

\* Electronic address: hartmann@theorie.physik.uni-goettingen.de; URL: <http://www.theorie.physik.uni-goettingen.de/~hartmann>

† Electronic address: peter@bartok.ucsc.edu; URL: <http://bartok.ucsc.edu/peter>; Temporary address: Department of Theoretical Physics, 1, Keble Road, Oxford OX1 3NP, England

<sup>1</sup> D. S. Fisher and D. A. Huse, *Ordered phase of short-range Ising spin-glasses*, Phys. Rev. Lett. **56**, 1601 (1986).

<sup>2</sup> D. S. Fisher and D. A. Huse, *Equilibrium behavior of the spin-glass ordered phase*, Phys. Rev. B **38**, 386 (1988).

<sup>3</sup> A. J. Bray and M. A. Moore, *Scaling theory of the ordered phase of spin glasses*, in *Heidelberg Colloquium on Glassy Dynamics and Optimization*, edited by L. Van Hemmen and I. Morgenstern (Springer, 1986), p. 121.

<sup>4</sup> W. L. McMillan, *Scaling theory of Ising spin glasses*, J. Phys. A **17**, 3179 (1984).

<sup>5</sup> A. J. Bray and M. A. Moore, *Lower critical dimension of Ising spin glasses: a numerical study*, J. Phys. C **17**, L463 (1984).

<sup>6</sup> W. L. McMillan, *Domain-wall renormalization-group study of the three-dimensional random Ising model*, Phys. Rev. B **30**, 476 (1984).

<sup>7</sup> A. K. Hartmann, *Scaling of stiffness energy for three-dimensional  $\pm J$  Ising spin glasses*, Phys. Rev. E **59**, 84

(1999).

<sup>8</sup> M. Palassini and A. P. Young, *Triviality of the ground state structure in Ising spin glasses*, Phys. Rev. Lett. **83**, 5126 (1999), (cond-mat/9906323).

<sup>9</sup> A. K. Hartmann, *Calculation of ground states of four-dimensional  $\pm J$  Ising spin glasses*, Phys. Rev. E **60**, 5135 (1999).

<sup>10</sup> K. Hukushima, *Domain-wall free energy of spin-glass models: Numerical method and boundary conditions*, Phys. Rev. E **60**, 3606 (1999).

<sup>11</sup> W. L. McMillan, *Domain-wall renormalization-group study of the two-dimensional random Ising model*, Phys. Rev. B **29**, 4026 (1984).

<sup>12</sup> H. Rieger, L. Santen, U. Blasum, M. Diehl, M. Jünger, and G. Rinaldi, *The critical exponents of the two-dimensional Ising spin glass revisited: exact ground-state calculations and Monte Carlo simulations*, J. Phys. A **29**, 3939 (1996).

<sup>13</sup> M. Palassini and A. P. Young, *Evidence for a trivial ground state structure in the two-dimensional Ising spin glass*, Phys. Rev. B **60**, R9919 (1999), (cond-mat/9904206).

<sup>14</sup> A. K. Hartmann and A. P. Young, *Lower critical dimension of Ising spin glasses*, Phys. Rev. B **64**, 180404 (2001), (cond-mat/0107308).

<sup>15</sup> A. C. Carter, A. J. Bray, and M. A. Moore, *Aspect-ratio scaling and the stiffness exponent  $\theta$  for Ising spin glasses*,

- Phys. Rev. Lett. **88**, 077201 (2002), (cond-mat/0108050).
- 16 A. J. Bray and M. A. Moore, *Chaotic nature of the spin-glass phase*, Phys. Rev. Lett. **58**, 57 (1987).
  - 17 A. A. Middleton, *Energetics and geometry of excitations in random systems*, Phys. Rev. B **63**, 060202(R) (2001), (cond-mat/0007375).
  - 18 G. Parisi, *Infinite number of order parameters for spin-glasses*, Phys. Rev. Lett. **43**, 1754 (1979).
  - 19 G. Parisi, *The order parameter for spin glasses: a function on the interval 0–1*, J. Phys. A. **13**, 1101 (1980).
  - 20 G. Parisi, *Order parameter for spin-glasses*, Phys. Rev. Lett. **50**, 1946 (1983).
  - 21 M. Mézard, G. Parisi, and M. A. Virasoro, *Spin Glass Theory and Beyond* (World Scientific, Singapore, 1987).
  - 22 F. Krzakala and O. C. Martin, *Spin and link overlaps in 3-dimensional spin glasses*, Phys. Rev. Lett. **85**, 3013 (2000), (cond-mat/0002055).
  - 23 M. Palassini and A. P. Young, *Nature of the spin glass state*, Phys. Rev. Lett. **85**, 3017 (2000), (cond-mat/0002134).
  - 24 H. G. Katzgraber, M. Palassini, and A. P. Young, *Monte Carlo simulations of spin glasses at low temperatures*, Phys. Rev. B **63**, 184422 (2001), (cond-mat/0108320).
  - 25 E. Marinari and G. Parisi, *On the effects of changing the boundary conditions on the ground state of Ising spin glasses*, Phys. Rev. B **62**, 11677 (2000).
  - 26 M. A. Moore, *Corrections to scaling in the droplet picture of spin glasses* (2002), (cond-mat/0203469).
  - 27 J. Lamarcq, J.-P. Bouchaud, O. C. Martin, and M. Mézard, *Non-compact local excitations in spin glasses* (2002), (cond-mat/0107544).
  - 28 S. Liang, *Application of cluster algorithms to spin glasses*, Phys. Rev. Lett. **69**, 2145 (1992).
  - 29 N. Kawashima, H. Hatano, and M. Suzuki, *Zero-temperature critical phenomena in two-dimensional spin glasses*, J. Phys. A **25**, 4985 (1992).
  - 30 N. Kawashima and M. Suzuki, *Replica optimization method for ground-state search of random spin systems*, J. Phys. A **25**, 1055 (1992).
  - 31 N. Kawashima and T. Aoki, *Zero-temperature critical phenomena in two-dimensional spin glasses*, J. Phys. Soc. Jpn. **69**, Suppl. A 169 (2000), (cond-mat/9911120).
  - 32 N. Kawashima, *Fractal droplets in spin glasses*, J. Phys. Soc. Jpn. **69**, 987 (2000), (cond-mat/9910366).
  - 33 M. Picco, F. Ritort, and M. Sales, *Statistics of lowest excitations in two dimensional Gaussian spin glasses* (2002), (cond-mat/0106554).
  - 34 A. K. Hartmann and H. Rieger, *Optimization Algorithms in Physics* (Wiley-VCH, Berlin, 2001).
  - 35 J. Houdayer, *A cluster Monte Carlo algorithm for 2-dimensional spin glasses*, Eur. Phys. J. B. **22**, 479 (2001).
  - 36 L. Bieche, J. P. Uhry, R. Maynard, and R. Rammal, *On the ground states of the frustration model of a spin glass by a matching method of graph theory*, J. Phys. A **13**, 2553 (1980).
  - 37 F. Barahona, *On the computational complexity of Ising spin glass models*, J. Phys. A **15**, 3241 (1982).
  - 38 R. G. Palmer and J. Adler, *Ground states of large samples of two-dimensional Ising spin glasses*, Int. J. Mod. Phys. C **10**, 667 (1999).
  - 39 The “world record” seems to be  $L = 1800$  in Ref. 38, while Ref. 14, which studied a large number of samples using readily available algorithms from the LEDA package, went up to size  $L = 480$ .
  - 40 We are grateful to M. A. Moore for a helpful discussion on this point.
  - 41 We should point out that there *are* polynomial algorithms for the  $d = 2$  Ising model with periodic boundary conditions. For example Saul and Kardar<sup>48,49</sup> (see also Ref. 50) were able to compute the partition function at finite- $T$  in polynomial time, but this method is not as efficient as the matching algorithm and so can only do rather small sizes, and, furthermore, it does not yield the ground state spin configuration. The more efficient transfer matrix approach of Merz and Chalker<sup>51</sup>, based on work by Cho and Fisher<sup>52</sup>, also unfortunately does not give the ground state spin configuration.
  - 42 Information about the spin glass ground state server at the University of Köln can be found at [http://www.informatik.uni-koeln.de/lis\\_juenger/projects/sgs.html](http://www.informatik.uni-koeln.de/lis_juenger/projects/sgs.html).
  - 43 J. Houdayer and O. C. Martin, *A geometrical picture for finite-dimensional spin glasses*, Europhys. Lett. **49**, 794 (2000).
  - 44 J. Houdayer, F. Krzakala, and O. C. Martin, *Large-scale low-energy excitations in 3-d spin glasses*, Eur. Phys. J. B. **18**, 467 (2000).
  - 45 The original definition of a sponge-like excitation<sup>43</sup> required the excitation to “wrap around” in *all* dimensions, which is only possible for  $d \geq 3$ . In two-dimensions, we feel it is convenient to use the same term for excitations comprising two domain walls which wrap around in one direction.
  - 46 W. H. Press, S. A. Teukolsky, W. T. Vetterling, and B. P. Flannery, *Numerical Recipes in C* (Cambridge University Press, Cambridge, 1995).
  - 47 M. Palassini, F. Liers, M. Jünger, and A. P. Young (2002), (manuscript in preparation.).
  - 48 L. Saul and M. Kardar, *Exact integer algorithm for the two-dimensional  $\pm J$  Ising spin glass*, Phys. Rev. E **48**, R3221 (1993).
  - 49 L. Saul and M. Kardar, *The 2d  $\pm J$  Ising spin glass: exact partition functions in polynomial time*, Nucl. Phys. B **432**, 641 (1994).
  - 50 T. Regge and R. Zecchina, *Exact solution of the Ising model on group lattices of genus  $g > 1$* , J. Math. Phys. **37**, 2796 (1996).
  - 51 F. Merz and J. T. Chalker, *Two-dimensional random-bond Ising model, free fermions, and the network model*, Phys. Rev. B **65**, 054425 (2002).
  - 52 S. Cho and M. P. A. Fisher, *Criticality in the two-dimensional random-bond Ising model*, Phys. Rev. B **55**, 1025 (1997).